Int. J. Electrochem. Sci., 11 **(2016)** 6356 – 6369, doi: 10.20964/2016.07.85

International Journal of ELECTROCHEMICAL SCIENCE
www.electrochemsci.org

Enhancement of Electrochemical Glucose Sensing by Using Multiwall Carbon Nanotubes decorated with Iron Oxide Nanoparticles

E.G. Uc-Cayetano[1], *L.C. Ordóñez*[2,*], *J.V. Cauich-Rodríguez*[1], *F. Avilés*[1]

[1] Centro de Investigación Científica de Yucatán, Unidad de Materiales, Calle 43 # 130, Col. Chuburná de Hidalgo, 97200 Mérida, Yucatán, México.
[2] Centro de Investigación Científica de Yucatán, Unidad de Energía Renovable, Carretera Sierra Papacal-Chuburná Puerto km. 5, 97302 Sierra Papacal, Yucatán, México.
[*]E-mail: lcol@cicy.mx

Received: 15 April 2016 / *Accepted:* 23 May 2016 / *Published:* 4 June 2016

The influence of iron oxide nanoparticles decorating the external surface of multiwall carbon nanotubes (MWCNTs) on the amperometric sensing of glucose in solution is investigated. Oxidized nanotubes are decorated with iron oxide nanoparticles and then glucose oxidase is chemically bound to the MWCNTs for glucose sensing within physiological levels. MWCNTs which are only oxidized (without decorating nanoparticles) are used as reference. The results of the electrochemical characterizations consistently show that the presence of iron oxide nanoparticles decorating the surface of MWCNTs enhance the amperometric response and the sensitivity to increments in glucose concentration, when compared to non-decorated MWCNTs. The biosensor containing iron oxide decorated nanoparticles showed an amperometric sensitivity of 4.75 μA/mMcm^2 and an average response time of 6.6 s.

Keywords: Carbon nanotubes, iron oxide, glucose sensing.

1. INTRODUCTION

Carbon nanotubes (CNTs) and other graphitic nanostructures such as graphene and expanded graphite are materials with extraordinary physical, physicochemical and electrochemical properties which are being aggressively investigated for a variety of sensing applications. Among many applications, they have been proposed as key materials for sensing of strain, moisture, gas, solvents, the presence of analytes and several biomolecules [1-5]. The physicochemical and electronic properties of CNTs along with their large aspect ratio, large surface-to-volume ratio and fast electrokinetics make them very attractive candidates for biosensing [1,2, 6]. Thus, sensing of biological molecules such as

proteins, DNA, glucose and other enzymes using either singlewall or multiwall carbon nanotubes (MWCNTs) has been widely reported [1, 4, 7-9]. In spite of the current progress in this area, the electrochemical response of CNTs used in a variety of sensing arrangements still needs to be improved. An alternative towards the continuous enhancement of this CNT electrochemical response is to chemically (or physically) modify its surface. In this regard, chemical oxidation (either by plasma or acid treatments) is a possible route to chemically activate the CNT surface [10, 11]. However, generation of OH, CO, and COOH functional groups at the CNT surface may not be enough for biosensing applications, and a few research efforts have suggested the use of metallic nanoparticles synergistically working with CNTs to achieve this aim [12-16]. It is expected that the use of metallic nanoparticles decorating CNTs may benefit the electron transfer and amperometric response of the sensor, improving also their electrocatalytic activity [13, 17-21]. In particular, the use of iron oxide nanoparticles seems to be a promising alternative given their small size, electric and magnetic properties [22, 23]. Several works have developed glucose sensing materials, arrangements and sensors using CNTs, see e.g. [1, 3, 4, 7]. Some of them have used nanoparticles such as silver, gold or boron [24-28] to enhance the sensor´s performance. The use of iron oxide nanoparticles in synergetic combination with other materials has been less reported [18, 29-32], and specific research on iron oxide decorated CNTs and their role in biosensing applications are scarce, see [33]. Therefore, this work investigates the role of iron oxide nanoparticles decorating the walls and ends of multiwall carbon nanotubes (MWCNTs) for their use as a glucose sensor. Details of the decoration procedure and physicochemical characterization of the decorated MWCNTs were reported in a previous publication [34], so the focus of the current work is on the electrochemical characterization of the novel sensing material, using as a reference chemically oxidized MWCNTs.

2. MATERIALS AND METHODS

2.1 Materials

Commercial MWCNTs (Cheap Tubes Inc., Brattleboro, USA) with purity >95 wt.%, outer diameter of 50-80 nm, inner diameter of 5-10 nm, and length ranging from 1-6 μm were used. The BET surface area of these MWCNTs is 110 m^2/g and the average Raman I_G/I_D intensity ratio is 0.89 [34]. Sulfuric acid (98.6 % v/v) and nitric acid (70 % v/v) used for the oxidation were purchased from J.T. Baker; triethylene glycol (TREG, 99 % v/v) was purchased from Sigma-Aldrich, iron (III) chloride hexahydrate (99 % v/v) and anhydrous sodium acetate (99 % w/w) used for the nanoparticle decoration were acquired from Merck. The enzyme used was glucose oxidase (GOx) from *Aspergillus niger* (≥100,000 units/g solid) in the form of lyophilized powder acquired from Sigma-Aldrich. N-(3-Dimethylaminopropyl)-N'-ethylcarbodiimide hydrochloride (EDAC), N-Hydroxysuccinimide (NHS), phosphate buffered saline (PBS), and D-(+)-Glucose (≥95%) were also acquired from Sigma-Aldrich.

2.2 Oxidation and decoration of carbon nanotubes

MWCNTs were first oxidized by an acid treatment before their decoration with iron oxide nanoparticles. Control samples were only oxidized. The MWCNT oxidation used a method based on a mixture of HNO_3 and H_2SO_4 as oxidizing agents which has been proven efficient in the generation of OH, CO and COOH functional groups on the MWCNT surface [10, 11]. This procedure, reported in [10], consisted in dispersing 0.3 g of MWCNTs in 70 mL of a mixture of 8.0 M HNO_3 (35 mL) and 8.0 M H_2SO_4 (35 mL), stirring for 15 min at 60 °C followed by 2 h of dispersion in an ultrasonic bath (100 W, 42 kHz). The oxidized MWCNTs were then washed with distilled water, filtered and dried at 100 °C for 12 h.

The method used for decorating MWCNTs with iron oxide nanoparticles consisted in ultrasonically dispersing 100 mg of oxidized MWCNTs in 50 mL of TREG for 1 h and then adding the metal precursor under reflux at 200 °C. After dispersion, 200 mg of $FeCl_3*6H_2O$ and 3.6 g of anhydrous sodium acetate were added to the solution. The resulting mixture was brought to reflux at 200 °C for 30 min. The obtained MWCNTs were then centrifuged with acetone, washed and filtered with distilled water and finally dried at 100 °C for 12 h.

2.3 Immobilization of glucose oxidase onto carbon nanotubes

GOx was immobilized over the surface of MWCNTs through amide bond formation by the reaction between the carboxylic functional groups of the oxidized MWCNTs and the amines groups of GOx. For this, 10 mg of MWCNTs were dispersed using an ultrasonic bath (100 W, 42 kHz) in 10 mL of deionized water for 1 h. Mechanical agitation at ~100 rpm for 5 min was then used, adding 20 mg of EDAC followed by 30 mg of NHS under a nitrogen atmosphere. Upon dissolution of EDAC and NHS, 8 mg of GOx were added maintaining the agitation for 24 h. The MWCNTs with immobilized GOx were then filtrated, washed with deionized water and stored at 3 °C. The immobilization was conducted on both oxidized only and oxidized and decorated MWCNTs.

2.4 Physicochemical and electrochemical characterization

MWCNTs were characterized by Fourier transform infrared spectroscopy (FT-IR) using a Nicolet Protege 460 equipment in a spectral range from 4,000 to 400 cm^{-1}. Spectra were obtained from KBr pellets containing a small amount of MWCNTs. Transmission electron microscopy (TEM) was carried out in a JEOL, JEM-2010F equipment operated at 80 kV.

Electrochemical measurements at room temperature were conducted using an Autolab PGSTAT 302 potentiostat-galvanostat. Measurements were carried out in a typical electrochemical three-electrode cell using a saturated calomel electrode (SCE, $Hg/Hg_2Cl_2/KCl$) as reference, and a graphite bar as the auxiliary electrode; each sample was deposited onto a 3 mm diameter glassy carbon (GC) disk, acting as the working electrode. Working electrodes were prepared by ultrasonically dispersing 10 mg of MWCNTs in 10 mL of deionized water and depositing 6 μL of the solution on the GC disk by using a micropipette. A scan rate of 50 mV/s was chosen for cyclic voltammetry (CV). The

CV cycles showed good reproducibility after the second cycle, and thus the third cycle was chosen as representative for CV. For chronoamperometry (CA) the potential was fixed at -0.5 V. For selected sensing experiments, 1.0 M PBS solution (pH=7.4) was used as electrolyte and D-(+)-glucose at different physiologically relevant concentrations was gradually added to the solution. Each experiment was repeated three to five times using different electrodes and representative curves are shown.

3. RESULTS AND DISCUSSION

3.1 Characterization of oxidized and decorated carbon nanotubes

3.1.1 Transmission electron microscopy

Oxidized MWCNTs and MWCNTs containing decorating nanoparticles are shown in Fig. 1a and 1b, respectively. The iron oxide nanoparticles are attached to the outer walls of the MWCNTs, as seen from Fig. 1b.

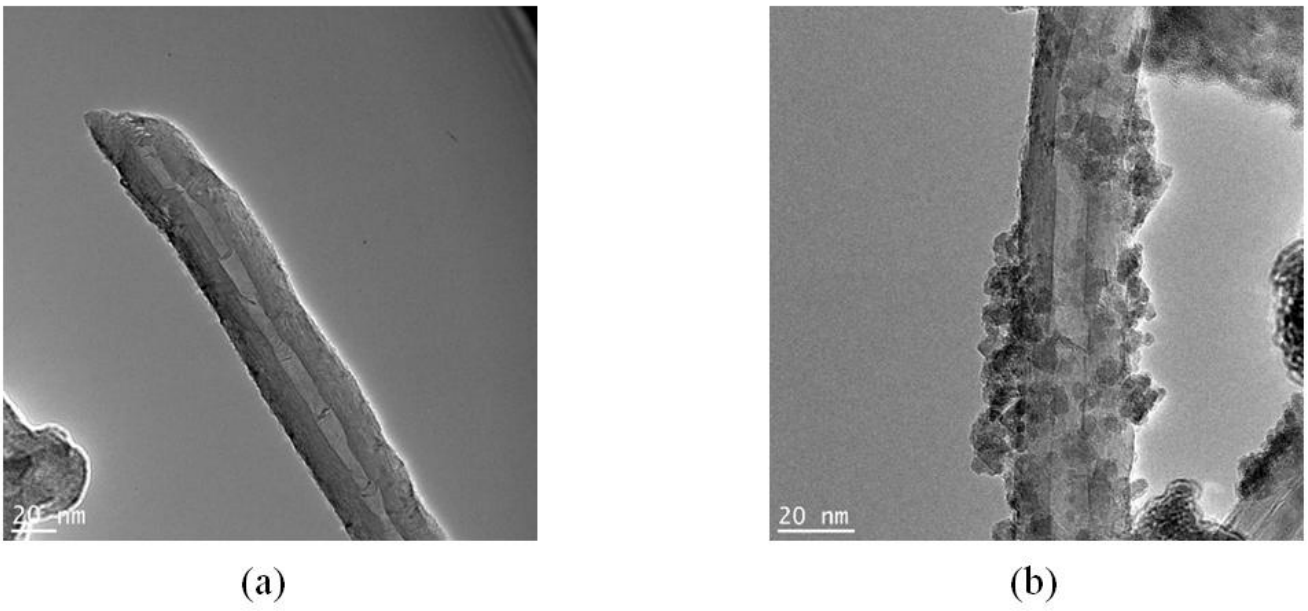

Figure 1. TEM images of treated MWCNTs. a) Oxidized only, b) oxidized and then decorated with iron oxide nanoparticles.

According to our previous research [34], the nanoparticles are dominantly Fe_3O_4 coexisting with Fe_2O_3 of 4-5 nm mean diameter; the estimated nanoparticle weight content is ~25% with respect to the weight of the MWCNTs. It has been suggested that bonding of iron oxide nanoparticles to the MWCNT walls is achieved by physical bonding and electrostatic attractions [35].

3.1.2 Cyclic voltammetry

Figure 2 shows the current density (*j)* as a function of the electrode potential (*E*) obtained by cyclic voltammograms of different electrodes in 1.0 M PBS solution at a scan rate of 50 mV/s. The neat GC electrode (*i*) shows very small current intensities and redox peaks are not distinguished in the -1.0 to 1.0 V range. The as-received MWCNTs (*ii*) show small reversible peaks in the range of -0.25 to -.035 V corresponding to the electrochemical processes of carbon [36] and to redox peaks of the metallic precursors/impurities used in the MWCNT synthesis, such as Ni and Co [37]. When the MWCNTs are acid oxidized (*iii*) the redox peaks corresponding to the metallic precursors vanishes, with the concomitant reduction in the current intensity. It is well known that such type of acid treatments not only introduce oxygen-containing functional groups but also purify the MWCNTs eliminating several metallic species left from their synthesis [38]. For the MWCNTs decorated with iron oxide nanoparticles (*iv*) the electrochemical behavior is markedly different. The current intensity largely increases due to the metallic particles and their corresponding redox pair is very marked at -0.2 V (cathodic) and -0.39 V (anodic), according to the reaction [37],

$$3\ FeO + H_2O \leftrightarrow Fe_3O_4 + 2\ H^+ + 2e^- \quad (1)$$

This behavior suggest that the iron oxide nanoparticles increase the electroactive surface area and mediate the electron transfer between electroactive species and the GC electrode, as has been recently pointed out [33].

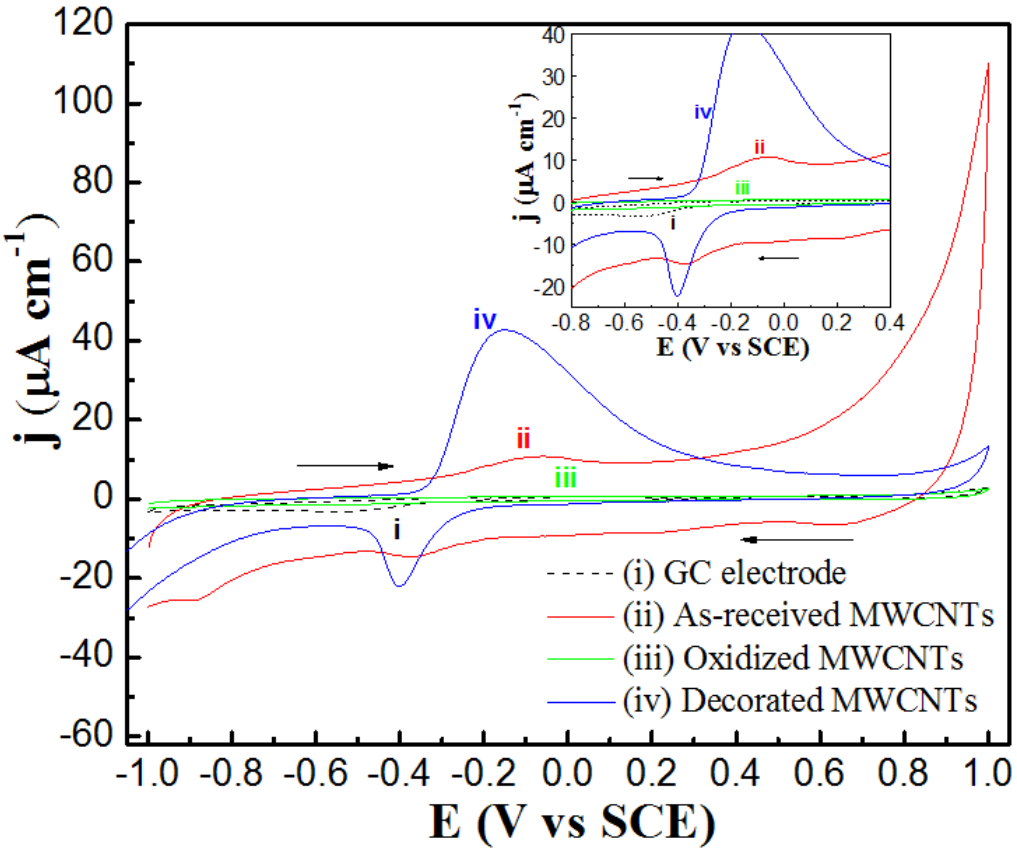

Figure 2. Cyclic voltammograms in PBS of the GC reference electrode (*i*), as-received MWCNTs (*ii*), oxidized MWCNTs (*iii*) and decorated MWCNTs (*iv*).

3.2 Glucose oxidase immobilization

3.2.1 Confirmation of glucose oxidase immobilization by FT-IR

Figure 3 shows the FT-IR analysis of the immobilization of glucose onto the MWCNTs. Figure 3a shows the FT-IR spectra of the oxidized MWCNTs and that of the GOx enzyme. The oxidized MWCNTs show absorption bands at 3000-3500 cm^{-1} and ~1400 cm^{-1}, which indicates the presence of hydroxyl functional groups; around 1600 cm^{-1} the vibration of the sp^2 carbon atoms is observed and C-H stretching is detected at 2920 and 2850 cm^{-1}. The vibration of carbonyl in carboxylic acids and C-O stretching is observed at ~1720 cm^{-1} and ~1110 cm^{-1}, respectively, see [10,39]. The GOx enzyme shows three absorption bands related to the peptide structure, assigned to amides I (1600-1700 cm^{-1}, C=O stretching vibration), II (1551 cm^{-1}, N-H bending) and III (1242 and 1244 cm^{-1}, C-N and C-H stretching and N-H torsion) [40]. Additionally, GOx shows the characteristic amide A (3400-3440 cm^{-1}) and amide B (2926 and 2928 cm^{-1}) bands, which originate from a Fermi resonance between the first overtone of amide II and the N-H stretching vibration [41].

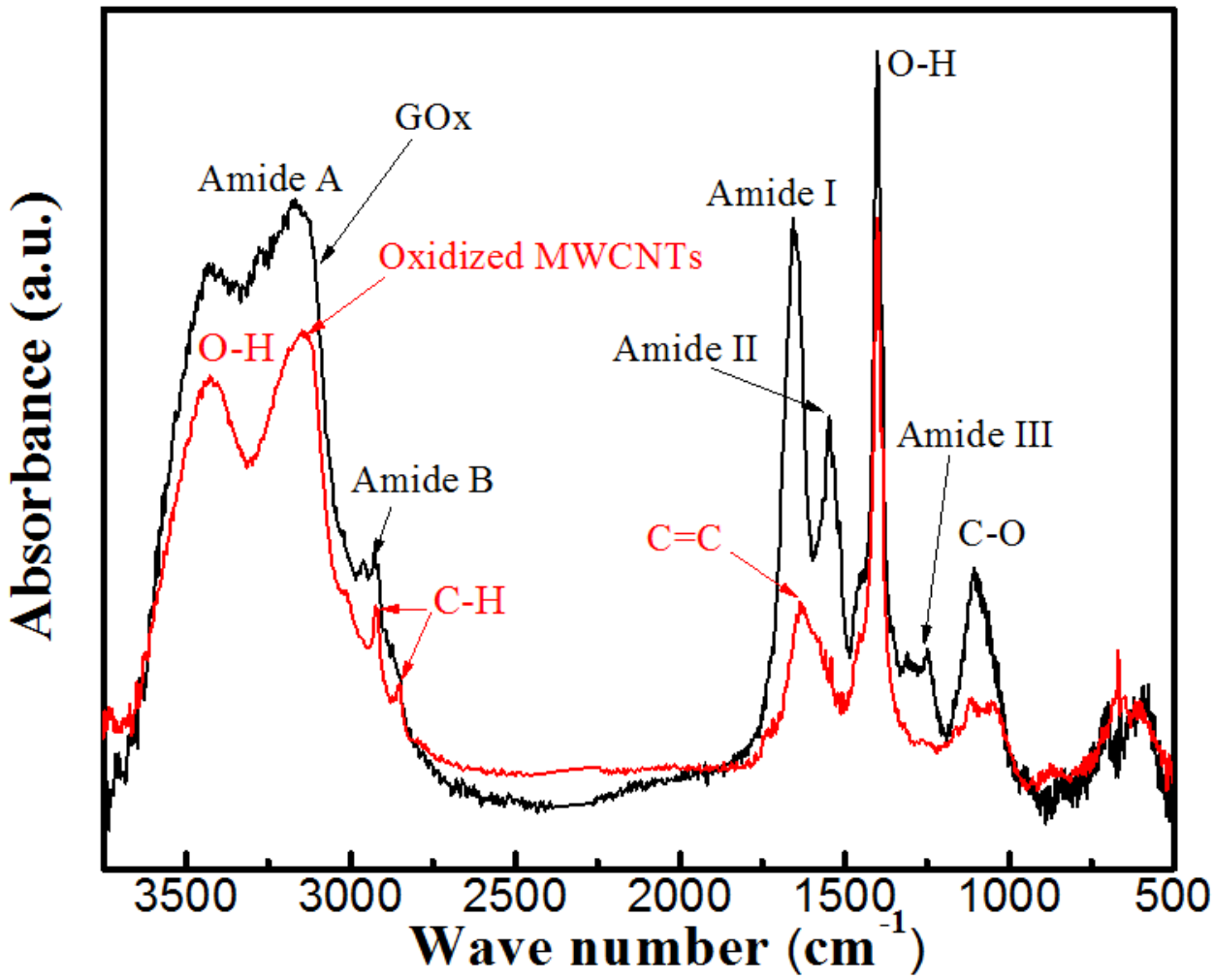

(a)

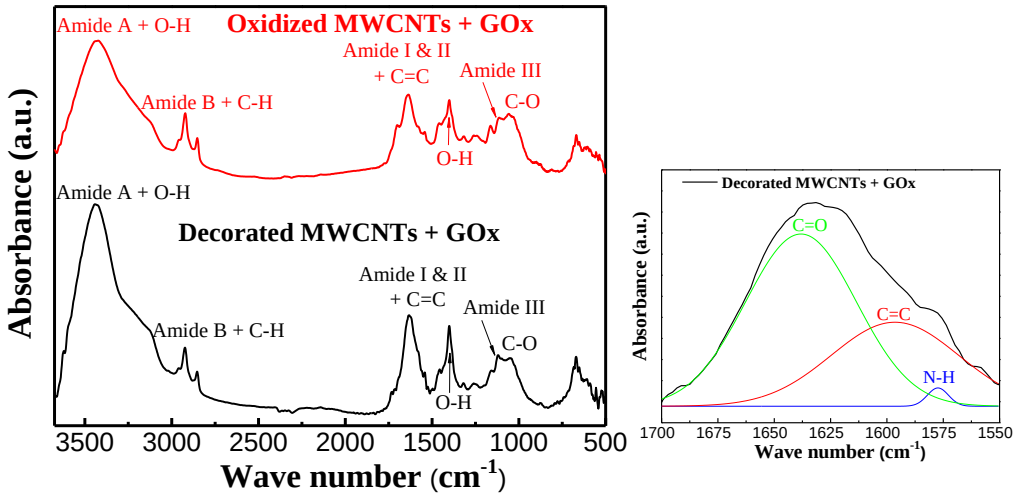

(b)

Figure 3. FT-IR analysis of GOx immobilization. a) Spectra of GOx and oxidized MWCNTs, b) spectra of oxidized and decorated MWCNTs containing immobilized GOx. A deconvolution of the spectrum of the decorated MWCNTs in the 1700-1550 cm^{-1} region is shown.

The spectra of the oxidized (upper plot) and decorated (lower plot) MWCNTs containing the immobilized GOx is shown in Fig. 3b. Some distinctive features are seen by comparing the spectra of the MWCNTs before GOx immobilization (Fig. 3a) to that after immobilization (Fig. 3b). The wide absorption band between 3000-3500 cm^{-1} increases its relative intensity and the two bands in this region observed in Fig. 3a merge to a single wide band centered at ~3400 cm^{-1}, indicating hydrogen bonding between the OH groups in the MWCNTs and the NH groups of the enzyme. Upon enzyme immobilization, the intensity of the CH groups at 1242 and 1244 cm^{-1} increases because of the amide III contribution and the OH band at ~1400 cm^{-1} and CO at ~1110 cm^{-1} of the MWCNTs broadens because of the GOx contribution. The spectrum of the decorated MWCNTs with the immobilized GOx is similar to that of the MWCNTs that were only oxidized, which indicates that the decoration with iron oxide nanoparticles leaves enough functional groups available to allow enzyme immobilization. The deconvolution of the 1700-1550 cm^{-1} broad band of the decorated MWCNTs containing immobilized GOx shows that such a band comprises C=C groups (~1600 cm^{-1}) belonging to the MWCNTs, and groups belonging to the enzyme (amide II ~1551 cm^{-1} and C=O ~1640 cm^{-1}), further indicating covalent bonding between GOx and the MWCNT surface for both, oxidized and decorated MWCNTs, see [42].

3.2.2 Electrochemical response of MWCNTs containing immobilized GOx

The CV response of oxidized and decorated MWCNTs containing immobilized GOx at 50 mV/s in PBS solution (pH=7.4) is shown in Fig. 4 for the interval of -1.0 to 1.0 V. Insets show a more detailed analysis in a narrower potential window of -0.7 V to -0.3 V, since the electron transfer

between the enzyme and the glucose in solution occurs at ~ -0.5 V [43]. Both, the oxidized MWCNTs with immobilized enzyme (Fig. 4a) and the decorated MWCNTs (Fig. 4b) show three redox peaks at ~ -0.5 V, 0.05-0.2 V and 0.5 V. The symmetric peak at -0.5 V (see inset) is characteristic of the GOx activity immobilized on MWCNTs [43-46]. This redox peak is related to the oxidation and reduction of GOx by the action of an electron transferred over its flavin adenine dinucleotide (FAD) group [44-47]. The exact position of this peak may depend on the pH of the solution [45,47]. The second and third redox peaks at 0.05-0.2 V and ~0.5 V are related to the enzyme oxidation and the oxidation of the MWCNT functional groups, see [44, 48].

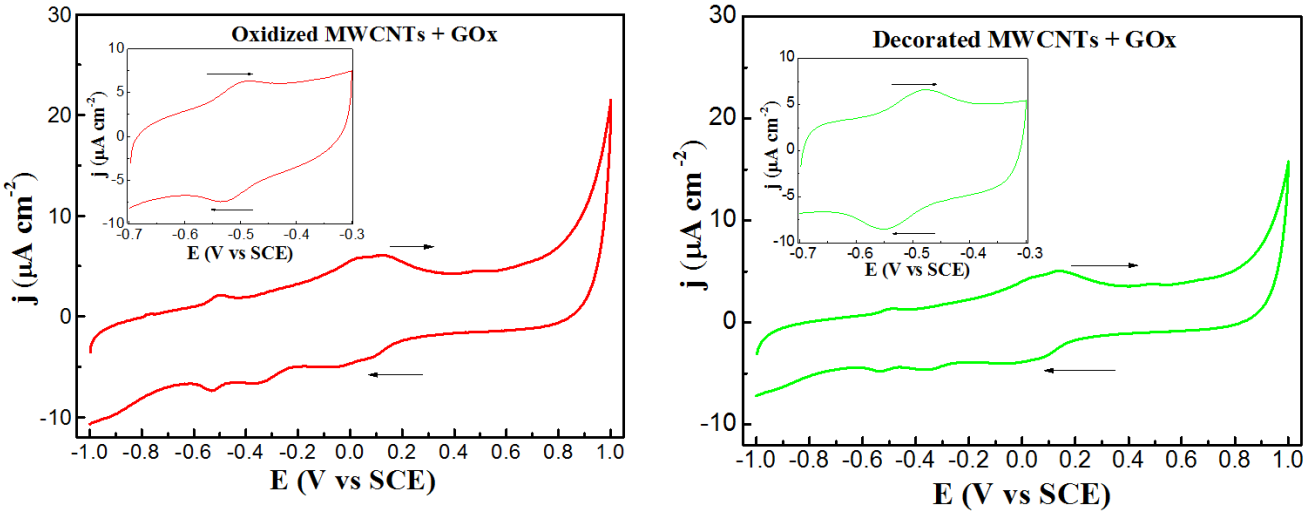

(a) (b)

Figure 4. Cyclic voltammograms in PBS of MWCNTs containing immobilized GOx. a) Oxidized MWCNTs, b) iron oxide decorated MWCNTs.

3.3 Glucose sensing

3.3.1 Glucose sensing by cyclic voltammetry

Glucose sensing was evaluated by CV for MWCNTs containing the immobilized GOx by immersing the working electrode in solutions containing 1, 2.5, 5 and 10 mM of D-(+)glucose in PBS. These concentrations are within the physiological levels found in healthy and diabetic persons, and they are sometimes expressed in mg/dL (1mM ≈ 18 mg/dL). Upon oxidation in presence of D-(+)glucose, the FAD group of GOx is expected to react producing gluconic acid and the hydroquinone form of FAD ($FADH_2$) [42]. Figure 5 shows the CV analysis in a -0.7 to -0.3 V potential window using a scan rate of 50 mV/s for oxidized (Fig. 5a) and decorated (Fig. 5b) MWCNTs. The curve corresponding to PBS is marked with *"i"*, and the four concentrations of glucose are marked with increasing roman numbers *"ii"* to *"v"*. All curves present an oxidation peak at -0.49 V and a reduction one at -0.54 V, shifted by 0.05 V. As seen from this figure the iron oxide nanoparticles yield a markedly different behavior in the performance of the glucose sensor since the curves corresponding to the decorated MWCNTs (Fig. 5b) present significantly higher current densities (*j*) than those of MWCNTs that were oxidized only (Fig. 5a).

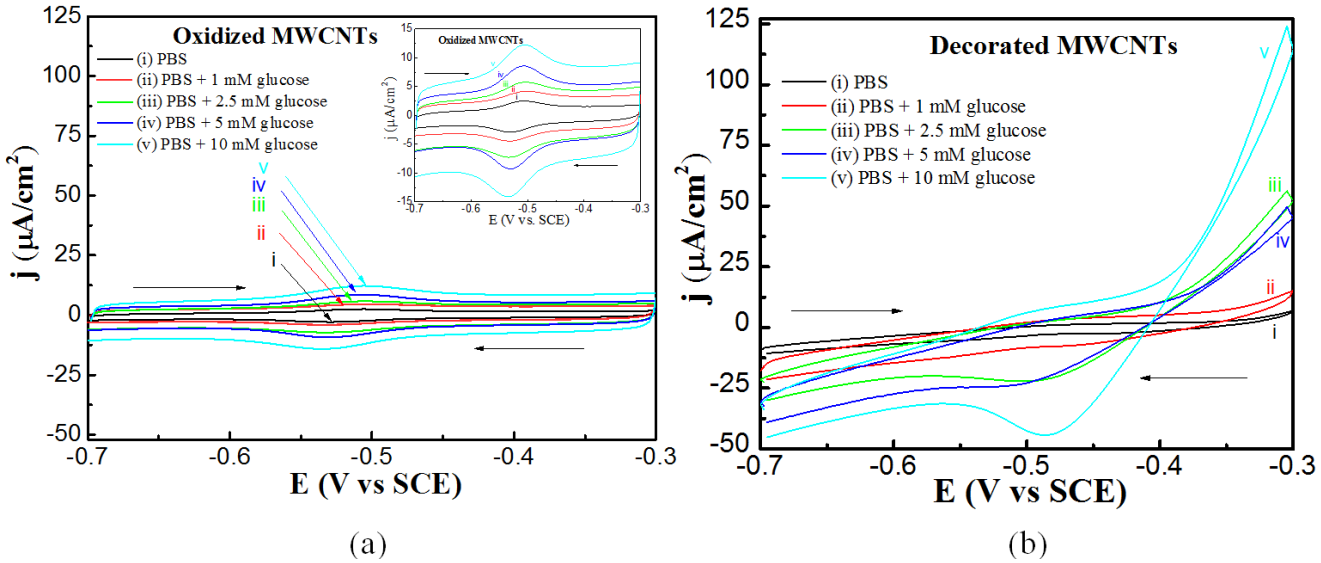

Figure 5. Cyclic voltammograms of MWCNTs containing immobilized GOx for increased concentrations of glucose in solution. a) Oxidized, b) iron oxide decorated.

To better capture this effect, Fig. 6 plots the normalized changes in the current density ($\Delta j/j_i$, where j_i is the initial current) as a function of the glucose concentration for five replicates of the experiment conducted in Fig. 5. The procedure was conducted for both currents, oxidation (Fig. 6a) and reduction (Fig. 6b).

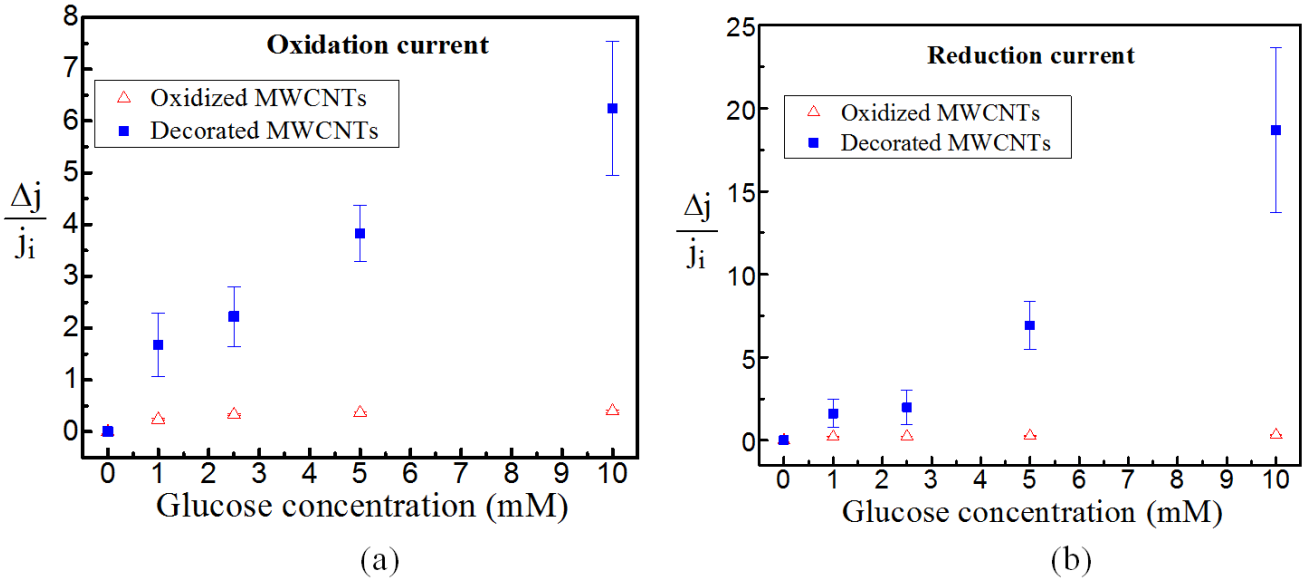

Figure 6. Normalized change in current density of oxidized and decorated MWCNTs upon increments in glucose concentration. a) Oxidation current, b) reduction current.

As seen from this figure, the changes in oxidation and reduction current densities are significantly higher when the MWCNTs are decorated with iron oxide nanoparticles than when the MWCNTs are only oxidized. The reduction current is more sensitive to changes in the glucose concentration than the oxidation one. By fitting a straight line to the data in Fig. 6 and using the area of the electrode (7.07 mm^2), the amperometric sensitivity can be found and such a parameter is listed in

Table 1 for both types of redox currents. For the oxidized MWCNTs the last data points significantly departed from linearity and hence were not considered in the data reported in Table 1. As seen from this table, the reduction current is more sensitive to the glucose concentration changes and the decorated MWCNTs render sensitivities that are ~8 times higher than that of the MWCNTs that were only oxidized, clearly indicating the paramount role of the iron oxide nanoparticles in the electron transfer.

Table 1. Amperometric sensitivity obtained by CV.

MWCNT treatment	Current type	Amperometric sensitivity ($\mu A/mMcm^2$)
Oxidized	Oxidation	0.33
	Reduction	0.61
Decorated	Oxidation	0.85
	Reduction	4.75

The amperometric sensitivity obtained (4.75 $\mu A/mMcm^2$) is high compared to other enzymatic sensors reported in the literature [13,25,28,29,49]. For example, Pang et al. [25] report a glucose sensitivity of 0.24 $\mu A/mMcm^2$ using MWCNT arrays decorated with Pt nanoparticles. Jose et al. [49] report a sensitivity of 0.47 $\mu A/mMcm^2$ for a mediator-free glucose oxidase-based carbon nanotube biosensor. However, a few other glucose sensors have reported very high sensitivity values, of the order of 100-200 $\mu A/mMcm^2$ [19,33].

3.3.2 Glucose sensing by chronoamperometry

Figure 7 shows the chronoamperometry analysis using PBS solutions containing glucose in concentrations of 1-10 mM at a constant potential of -0.5 V. The dynamic evolution of the electrical current for both, oxidized (Fig. 7a) and decorated (Fig. 7b) MWCNTs increases as the concentration of glucose increases. This is more clearly seen in Figs. 7c (for oxidized MWCNTs) and 7d (for decorated MWCNTs) where the steady current for electrocatalytic oxidation increases upon addition of glucose, yielding a stepwise amperometric response. The time required to reach a steady state electrical current can be obtained from a closer look of the curves in Figs. 7a and 7b, such as those shown at the corresponding insets. From such analysis, the average time required to reach 97% of the steady state current value in the 1-10 mM glucose concentration range was 8.6 s for the oxidized MWCNTs and 6.6 s for the iron oxide decorated MWCNTs. This indicates a fast stable response of the MWCNT modified electrode (see e.g., Li et al. [18] and Masoomi-Godarzi et al. [33]), which is enhanced by the decoration of MWCNTs with iron oxide nanoparticles.

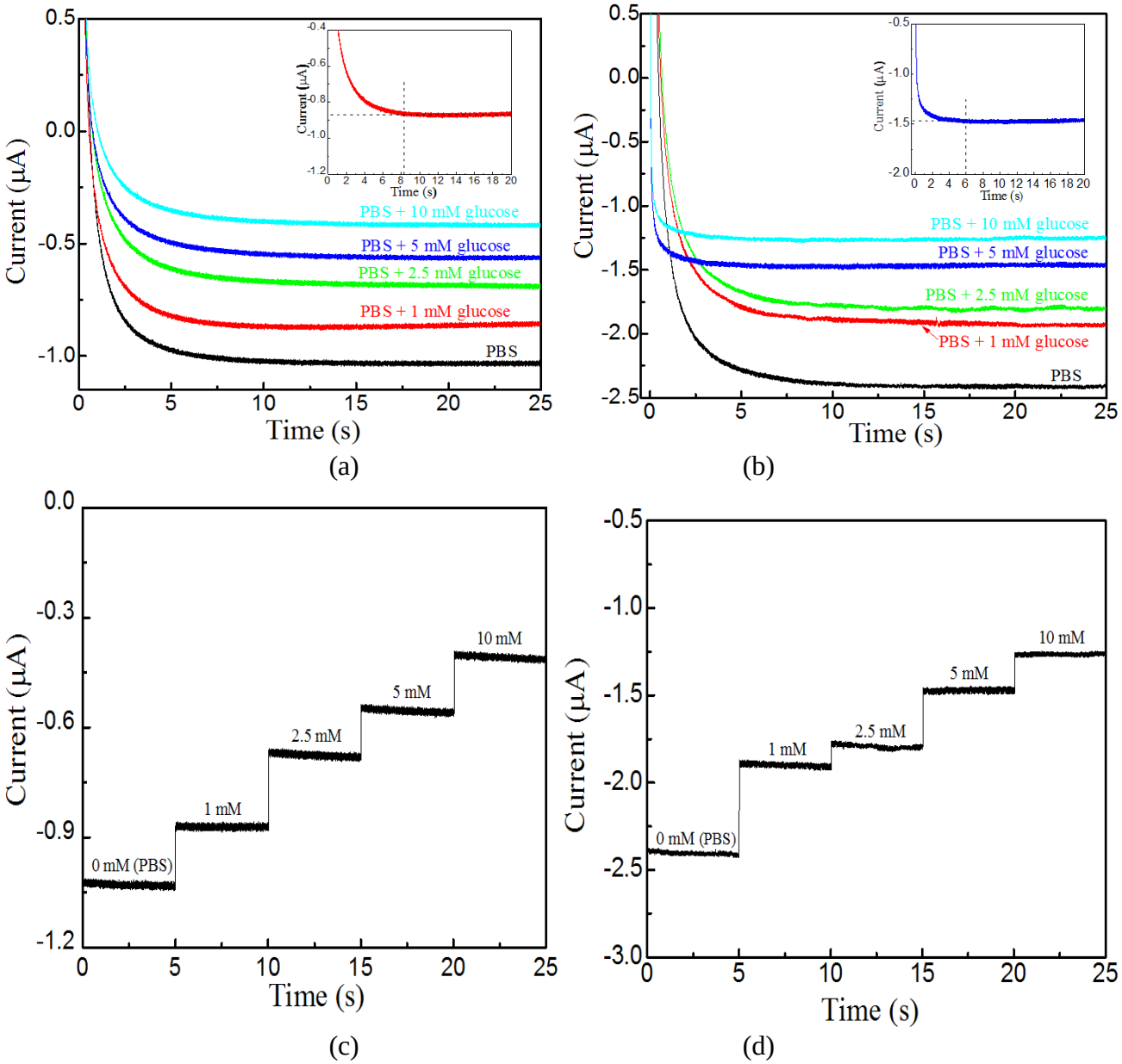

Figure 7. Amperometric response of MWCNT modified electrodes in PBS/glucose solutions with increased glucose concentrations. a) Current evolution for oxidized MWCNTs, b) current evolution for decorated MWCNTs, c) steady state currents for oxidized MWCNTs, d) steady state currents for decorated MWCNTs.

The maximum sensitivity and response time obtained for the developed sensor is summarized in Table 2, along with other published results. As seen from this Table, the sensors developed by Hrapovic et al. [13], Pang et al. [25] and Jose et al. [49], present less sensitivity than that developed herein; although working with a different sensing principle, a few other works such as those of Chen et al. [19], Zhang et al. [28], Kaushik et al. [29] and Masoomi-Gordazi et al. [33] have obtained higher sensitivities, and similar response times.

Table 2. Sensitivity and response time of the glucose sensor developed herein and compared to those of other authors.

Reference	Sensitivity (μA/mMcm^2)	Response time (s)
This work	4.75	6.6
[13]	2.11	3
[19]	112	5
[25]	0.24	3
[28]	16.6	Not reported
[29]	9.3	5
[33]	238.7	Not reported
[49]	0.47	Not reported

4. CONCLUSIONS

MWCNTs with immobilized glucose oxidase were used for electrochemical sensing of glucose in PBS solutions. Two types of MWCNTs were evaluated, viz. MWCNTs which were only oxidized by an acid treatment and MWCNTs whose outer walls were decorated with ~25% w/w iron oxide nanoparticles of 4-5 nm mean diameter. The covalent immobilization of glucose over the MWCNTs was proved by FT-IR analysis, and it was shown that the decoration with iron oxide nanoparticles does not disturb the enzyme immobilization. An amperometric sensitivity of 0.61 μA/mMcm^2 was measured for the oxidized MWCNTs by cyclic voltammetry, while the decorated MWCNTs showed a sensitivity of 4.75 μA/mMcm^2. The glucose biosensor exhibits a reproducible response with an average response time of 8.6 s for the oxidized MWCNTs and 6.6 s for the decorated ones. Therefore, it is concluded that the use of iron oxide nanoparticles decorating the MWCNT surface enhance the electron transfer and mass transport at the interface with the electrode, increasing the sensitivity and reducing the response time of the biosensor.

ACKNOWLEDGEMENTS
This research was supported by CONACYT (Mexico) through projects No. 220513 (FA) and CIAM No. 188089 (FA). Support in the form of a grant to our graduate school program from the "Fondo Mixto CONACYT-Gobierno del Estado de Yucatán", project No. 247046, is also acknowledged. Technical assistance from Alejandro May and Rossana Vargas from CICY is greatly appreciated.

References

1. S. K. Vashist, D. Zheng, K. Al-Rubeaan, J. H. T. Luong, F. S. Sheu, *Biotechnol. Adv.*, 29 (2011) 169.
2. A. T. Yousefi, S. Bagheri, N. A. Kadri, M. R. Mahmood, S. Ikeda, *Int. J. Electrochem. Sci.*, 10 (2015) 4183.
3. Y. Lin, F. Lu, Y. Tu, Z. Ren, *Nano Lett.*, 4 (2004) 191.
4. C. B. Jacobs, M. J. Peairs, B. J. Venton, *Anal. Chim. Acta*, 662 (2010) 105.
5. R. Leghrib, T. Dufourb, F. Demoisson, N. Claessens, F. Reniers, E. Llobet, *Sensor Actuat. B-Chem.*, 160 (2011) 974.

6. D. Vairavapandian, P. Vichchulada, M. D. Lay, *Anal. Chim. Acta*, 626 (2008) 119.
7. S. G. Wang, Q. Zhang, R. Wang, S. F. Yoon, J. Ahn, D.J. Yang, J.Z. Tian, J.Q. Li, Q. Zhou, *Electrochem. Commun.*, 5 (2003) 800.
8. A. I. Gopalan, K. P. Lee, D. Ragupathy, S. H. Lee, J.W. Lee, *Biomaterials*, 30 (2009) 5999.
9. Y. Liu, M. Wang, F. Zhao, Z. Xu, S. Dong, *Biosens. Bioelectron.*, 21 (2005) 984.
10. F. Avilés, J.V. Cauich-Rodríguez, L. Moo-Tah, A. May-Pat, R. Vargas-Coronado, *Carbon*, 47 (2009) 2970.
11. V. Datsyuk, M. Kalyva, K. Papagelis, J. Parthenios, D. Tasis, A. Siokou, I. Kallitsis, C. Galiotis, *Carbon*, 46 (2008) 833.
12. S. Liu, H. Ju, *Biosens. Bioelectron.*, 19 (2003) 177.
13. S. Hrapovic, Y. Liu, K. B. Male, J. H. T. Luong, *Anal. Chem.*, 76 (2004) 1083.
14. X. Kang, Z. Mai, X. Zou, P. Cai, J. Mo, *Talanta*, 74 (2008) 879.
15. A. K. Johnson, A. M. Zawadzka, L. A. Deobald, R. L. Crawford, A. J. Paszczynski, *J. Nanopart. Res.*, 10 (2008) 1009.
16. Y. Yu, Z. Chen, S. He, B. Zhang, X. Li, M. Yao, *Biosens. Bioelectron.*, 52 (2014) 147.
17. J. Xu, X. W. Wei, X. J. Song, X. J. Lu, C. C. Ji, Y. H. Ni, G. C. Zhao, *J. Mater. Sci.*, 42 (2007) 6972.
18. J. Li, R. Yuan, Y. Chai, X. Che, *J. Mol. Catal. B-Enzym.*, 66 (2010) 8.
19. K. J. Chen, C. F. Lee, J. Rick, S. H. Wang, C. C. Liu, X. J. Hwang, *Biosens. Bioelectron.*, 33 (2012) 75.
20. K. Zargoosh, M. J. Chaichi, M. Shamsipur, S. Hossienkhani, S. Asghari, M. Qandalee, *Talanta*, 93 (2012) 37.
21. P. Clément, I. Hafaiedh, E. J. Parra, A. Thamri, J. Guillot, A. Abdelghani, E. Llobet, *Carbon*, 78 (2014) 510.
22. T. Tabakova, D. Andreeva, V. Idakiev, A. Andreev, R. Giovanoli, *J. Mater. Sci.*, 31 (1996) 1101.
23. A. K. Gupta, M. Gupta, *Biomaterials*, 26 (2005) 3995.
24. L. Q. Rong, C. Yang, Q. Y. Qian, X. H. Xia, *Talanta*, 72 (2007) 819.
25. X. Pang, D. He, S. Luo, Q. Cai, *Sensor Actuat. B-Chem.*, 137 (2009) 134.
26. J. Lin, C. He, Y. Zhao, S. Zhang, *Sensor Actuat. B-Chem.*, 137 (2009) 768.
27. C. Deng, J. Chen, X. Chen, C. Xiao, L. Nie, S. Yao, *Biosens. Bioelectron.*, 23 (2008) 1272.
28. H. Zhang, Z. Meng, Q. Wang, J. Zheng, *Sensor Actuat. B-Chem.*, 158 (2011) 23.
29. A. Kaushik, R. Khan, P. R. Solanki, P. Pandey, J. Alam, S. Ahmad, B. D. Malhotra, *Biosens. Bioelectron.*, 24 (2008) 676.
30. L. Yang, X. Ren, F. Tang, L. Zhang, *Biosens. Bioelectron.*, 25 (2009) 889.
31. F.N. Comba, M. D. Rubianes, P. Herrasti, G. A. Rivas, *Sensor Actuat. B-Chem.*, 149 (2010) 306.
32. T. T. Baby, S. Ramaprabhu, *Talanta*, 80 (2010) 2016.
33. S. Masoomi-Gordazi, A. A. Khodadadi, M. Vesali-Naseh, Y. Mortazavi, *J. Electrochem. Soc.*, 161 (2014) B19.
34. E. G. Uc-Cayetano, F. Avilés, J. V. Cauich-Rodríguez, R. Schönfelder, A. Bachmatiuk, M. H. Rümmeli, F. Rubio, M. P. Gutierrez-Amador, G. J. Cruz, *J. Nanopart. Res.*, 16 (2014) 2192.
35. J. Lu, *Carbon*, 45 (2007) 1599.
36. S. Minnikanti, P. Skeath, N. Peixoto, *Carbon*, 47 (2009) 884.
37. M. Pourbaix, *Atlas of electrochemical equilibria in aqueous solutions*, National Association of Corrosion Engineers, International Cebelcor, Houston, TX (1974).
38. P. X. Hou, C. Liu, H. M. Cheng, *Carbon*, 46 (2008) 2003.
39. R. Schönfelder, F. Avilés, A. Bachmatiuk, J. V. Cauich-Rodriguez, M. Knupfer, B. Büchner, M. H. Rümmeli, *Appl. Phys. A-Mater*, 106 (2011) 843.
40. P. Singh, S. Benjakul, S. Maqsood, H. Kishimura, *Food Chem.*, 124 (2011) 97.
41. G. Wille, M. Ritter, R. Friedemann, W. Mäntele, G. Hübner, *Biochemistry-US*, 42 (2003) 14814.
42. P. Wu, Q. Shao, Y. Hu, J. Jin, Y. Yin, H. Zhang, C. Cai, *Electrochim. Acta*, 55 (2010) 8606.

43. W. Grosse, J. Champavert, S. Gambhir, G. G. Wallace, S. E. Moulton, *Carbon*, 61 (2013) 467.
44. M. R. Guascito, D. Chirizzi, C. Malitesta, E. Mazzotta, *Analyst*, 136 (2011) 164.
45. C. Cai, J. Chen, *Anal. Biochem.*, 332 (2004) 75.
46. M. Moumene, D. Rochefort, M. Mohamedi, *Int. J. Electrochem. Sci.*, 8 (2013) 2009.
47. B. C. Janegitz, R. Pauliukaite, M. E. Ghica, C. M. A. Brett, O. Fatibello-Filho, *Sensor Actuat. B-Chem.*, 158 (2011) 411.
48. K. Kinoshita, *Carbon: Electrochemical and Physicochemical Properties*, John Wiley Sons, New York (1998).
49. M. V. Jose, S. Marx, H. Murata, R. R. Koepsel, A. J. Rusell, *Carbon*, 50 (2012) 4110.